

# **Diffraction imagery of a degraded edge object in presence of image motions**

AMI CHANDRA, R. N. SINGH, K. SINGH

Physics Department, Indian Institute of Technology, Delhi, Haus Khas, New Delhi 110016,  
India.

Diffraction images of incoherently illuminated degraded edge in the presence of image motions have been studied theoretically. The degrading effects of transverse and longitudinal sinusoidal vibrations and linear and parabolic image motions have been studied separately. Intensity distribution in diffraction images has been calculated using the transfer function approach. The results have been presented graphically. It has been observed that the consideration of edge degradation effect is much important where the effects of various types of image motions on the performance of optical systems are to be evaluated.

## **1. Introduction**

Image formation by optical system in the presence of disturbing effects of aberrations and other constructional defects has been well studied. The sources of external disturbances, such as various types of image motions, are very important in aerial reconnaissance photography [1], and in space optics [2-4]. Despite the application of image motion compensation techniques there always remain some residual image motions. Motion degradation in the imagery has, therefore, been one of the important areas of concern in space photography and astronomy. The evaluation of the amount and types of motion degradation is desirable in the assessment of operational performance of optical systems and in the design of image enhancement techniques, because the enhancement of imagery usually requires some knowledge of the amount and type of degradation introduced in the image. This is also important in the image

restoration by post-exposure manipulation [5] and in the design of airborne cameras [6-8]. Considerations of image motions are also important while dealing with the systems to assess the performance of earth resources remote sensors [9]. The philosophical and technical implications of MTF analysis techniques, as related to the prediction and measurement of photographic and electro-optical system performance, are considered by WELCH [10]. Various types of image motions of interest are: i) linear, ii) parabolic, iii) transverse and longitudinal sinusoidal vibrations, and iv) random motion. A good account of various types of motion is given by JENSEN [11]. A comprehensive bibliography concerning the work on image formation in the presence of various types of image motions can be found elsewhere [1, 11-14]. More recently PHAUJDAR et al. [15] have evaluated the complex transfer function for both quadratic and uniformly accelerated relative motion which superimposed oscillations. Image degradation due to the random motion has been studied by MAHAJAN [16] and the results are tantamount to those obtained by SINGH and DHILLON [17] for diffraction of Gaussian correlated partially coherent radiation by an annular aperture.

In view of the above discussion, it becomes clear that the calculations of imagery of various objects in the presence of image motion are of considerable interest [11-13]. An edge object does not possess any characteristic dimensions and many of the other objects encountered in practice may also be considered as a collection of edge objects with different orientations, contrasts and sharpnesses. Therefore, edge objects find a prominent place among various test targets. The edge spread function is also a valuable concept in the image evaluation of optical systems. The MTF evaluation using edge trace analysis technique has, for example, been used to assess the image motion compensation capabilities of lunar orbiter photographic system in actual operation and preflight laboratory testing [18]. The investigations of MTF analysis technique, with particular emphasis on edge gradient analysis, are useful in prediction and measurement of operation system performance. These objects are also of considerable importance in connection with Mach effect [19]. Investigations on the edge image have, therefore, been a subject of much theoretical and experimental research. Some of the papers on the subject are due to BARAKAT [20,21], RATTAN and SINGH [22], SHEPPARD and CHOUDHURY [23], GUPTA and SINGH [23], and WILSON [25].

In most of the investigations regarding edge image analysis, sharp edge objects have been considered. However, in practice, the edge may not be ideal, but degraded to various amounts due to limitations in generating these objects. KINZLY [26] has, therefore, studied the im-

agery of degraded edge objects illuminated by partially coherent light. The use of high as well as low contrast edges as test targets for determining the linearity of optical instruments has also been suggested by KINZLY [27]. Imaging equations for a simple microdensitometer using quasi-monochromatic partially coherent illumination have also been developed [28].

The assessment of optical systems with the edge trace analysis will not be free from errors if the edge employed is not ideally sharp. The results will depend upon the amount of degradation present in the edge.

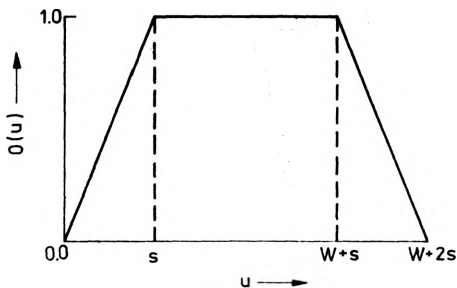
In view of what has been said above, we have theoretically studied the diffraction imagery of degraded edge by an optical system in presence of transverse and longitudinal sinusoidal vibrations and also in presence of linear and parabolic image motions. The object illumination has been considered to be incoherent.

## 2. Theory

The distribution of intensity transmittance in an incoherently illuminated object can be written as (Fig. 1):

$$O(u) = \begin{cases} 0.0 & u \leq 0 \\ u/s & 0 < u \leq s \\ 1.0 & s < u \leq W + s \\ \frac{(W + 2s - u)}{s} & W + s < u \leq W + 2s \\ 0.0 & u > W + 2s \end{cases} \quad \text{for} \quad (1)$$

where  $u$ ,  $W$  and  $s$  are expressed in diffraction units and considered in the direction of variation of intensity transmittance. The reduced



distance  $u$  is related to the actual distance  $x$  by the relation  $u = \pi x / \lambda F$ , where  $\lambda$  is the wavelength of light used, and  $F$

Fig. 1. Intensity distribution in the degraded edge-object

is the  $f$ -number of the optical system;  $W$  much longer than unity means a degraded edge.

The spatial frequency spectrum of the object is the Fourier transform of the object intensity distribution

$$O(\omega) = \int_{-\infty}^{+\infty} O(u) \exp[-i u \omega] du, \quad (2)$$

where  $\omega$  is the dimensionless spatial frequency. By inserting  $O(u)$  from Eq. (1) into Eq. (2) and after simplification, it turns out to be

$$O(\omega) = 4 \sin \frac{\omega s}{2} \sin \frac{\omega W}{2} (W + s) \exp\left[-i\omega \left(\frac{W}{2} + s\right)\right] / s\omega^2. \quad (3)$$

Now, the frequency spectra of the object and image are related by the optical transfer function of the imaging system as

$$I(\omega) = O(\omega) T(\omega). \quad (4)$$

The intensity distribution in the image of an incoherently illuminated one-dimensional object is the inverse Fourier transform of  $I(\omega)$ , i.e.

$$I(v) = \int_{-2}^2 T(\omega) O(\omega) \exp[i v \omega] d\omega, \quad (5)$$

which after substitution of  $O(\omega)$  gives

$$I(v) = 4 \int_{-2}^2 T(\omega) \frac{\sin \omega s / 2}{s \omega^2} \sin \frac{\omega W}{2} (W + s) \exp\left[\frac{i\omega}{2} (2v - W - 2s)\right] d\omega. \quad (6)$$

Here  $v$  is the distance in the image plane in the diffraction units. It is well known that the intensity is a real quantity. Therefore, taking the real part of Eq. (6), we may write

$$I(v) = \frac{8}{s} \int_0^2 T(\omega) \frac{\sin \omega s / 2}{\omega^2} \sin \frac{\omega W}{2} (W + s) \cos\left[\frac{\omega}{2} (2v - 2s - W) + \theta\right] d\omega, \quad (7)$$

where  $\theta$  is the phase angle in case of parabolic motion. Now the transfer function  $T(\omega)$  of the space invariant system in the presence of image motion, except for the case of longitudinal vibrations, can be written as

$$T(\omega) = D(\omega) t(\omega), \quad (8)$$

where  $D(\omega)$  is the transfer function of the optical system, and for a diffraction limited system with circular aperture it is given by

$$D(\omega) = \frac{2}{\pi} \left[ \cos^{-1} \frac{\omega}{2} - \frac{\omega}{2} \left( 1 - \frac{\omega^2}{4} \right)^{1/2} \right]. \quad (9)$$

The transfer function  $t(\omega)$  of different types of motion is known [1, 29-31]. For linear image motion, it is written as

$$t(\omega) = \text{sinc}(\pi A \omega) \exp(-i \pi A \omega), \quad (10)$$

where  $A = (vt_e/2\lambda F)$  is the motion parameters,  $t_e$  is the interval of exposure, and  $v$  is the relative linear velocity of the image plane. For transverse sinusoidal vibrations, it is written as

$$t(\omega) = J_0(\pi A \omega), \quad (11)$$

where  $J_0$  is the Bessel function of zero-order and first kind.  $A = 2f\theta_m/\lambda F$ , where  $\theta_m$  is the amplitude of angular displacement of the image and  $F$  is the f-number of the imaging system. The transfer function for the parabolic motion is given by

$$t(\omega) = \frac{(I_1^2 + I_2^2)^{1/2}}{2(\omega A)^{1/2}} \exp\{i \tan^{-1}(I_2/I_1)\}. \quad (12)$$

Here the motion parameter  $A = Bt_e^2/2\lambda F$ ,  $B$  is a constant, and  $I_1$  and  $I_2$  are the well-known Fresnel's integrals given by

$$I_1 = \int_0^{2\sqrt{A\omega}} \cos(\pi u^2/2) du \quad \text{and} \quad I_2 = \int_0^{2\sqrt{A\omega}} \sin(\pi u^2/2) du.$$

The transfer function of longitudinal vibrations cannot be expressed by the product of two functions [30], but is written as

$$T(\omega) = \frac{4}{\pi} \int_0^{1-\omega/2} J_0\left(\pi \bar{E}_1 \frac{\omega \xi}{2}\right) \left\{ 1 - (\xi + \omega/2)^2 \right\}^{1/2} \cos\left(\pi \bar{E}_0 \frac{\omega \xi}{2}\right) d\xi, \quad (13)$$

where  $\bar{E}_1$  is the amplitude of vibrations and  $\bar{E}_0$  represents the average amount of defocussing of the image plane, both  $\bar{E}_1$  and  $\bar{E}_0$  being expressed in diffraction units.

### 3. Results and discussion

Intensity distributions in the image of a degraded edge (i.e.,  $W \gg 1$ ) in the presence of various types of image motion have been evaluated using Eq. (7). Due to the presence of highly oscillatory trigonometric functions, the integral was divided into eight parts and then evaluated by high order Gauss quadrature method using 40-Gauss points. Our results in the case of an ideal edge for various amounts of image

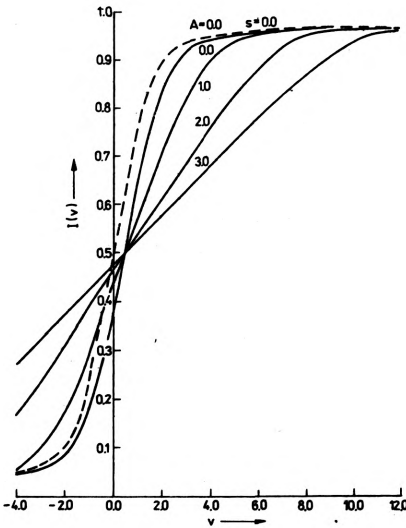


Fig. 2. Intensity distribution in the image of degraded edge ( $s = 1.0$ ) in the presence of linear image motion. Linear phase put in  $T(\theta)$  has been neglected.

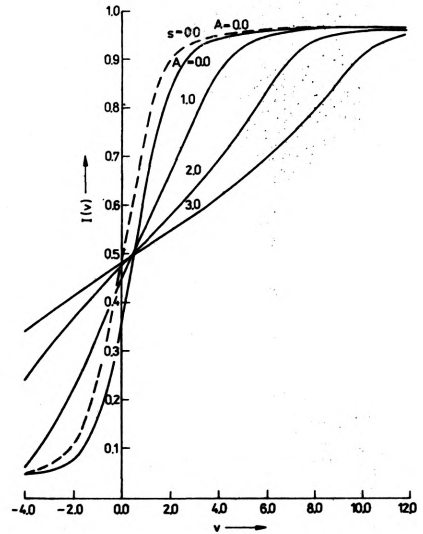


Fig. 3. The same as in Fig. 2, but in the presence of transverse vibrations.

motion agree with those published by RATTAN and SINGH [22], while the results of degraded edge in the absence of any image motion agree with those of KINZLY [26]. The usual criterion for normalization, i.e.,  $I(-\infty) = 0.0$ , and  $I(\infty) = 1.0$ , requires the knowledge of the area under the irradiance curve which is tedious to calculate. Hence, the intensity at the centre of the geometrical edge, i.e.,  $v = W/2$ , has been taken as unity for the purpose of normalization.

Figures 2-5 show the normalized intensity in the image of a degraded edge with the degradation parameters  $s = 1.0$  and afflicted by various amounts of linear motion, transverse and longitudinal sinusoidal

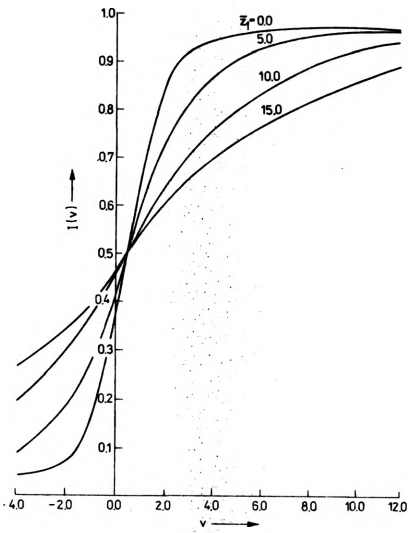


Fig. 4. The same as in Fig. 2, but in presence of longitudinal vibrations

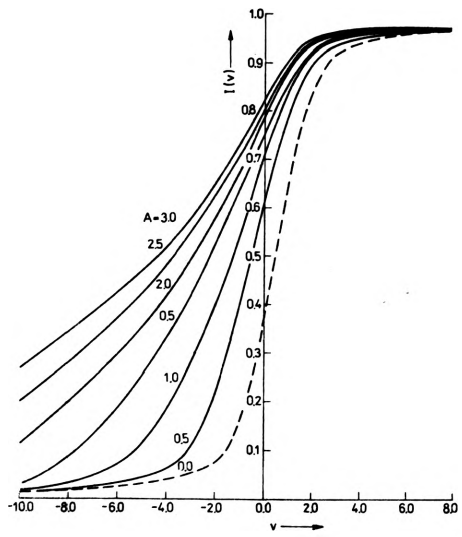


Fig. 5. The same as in Fig. 2, but in presence of parabolic image metric

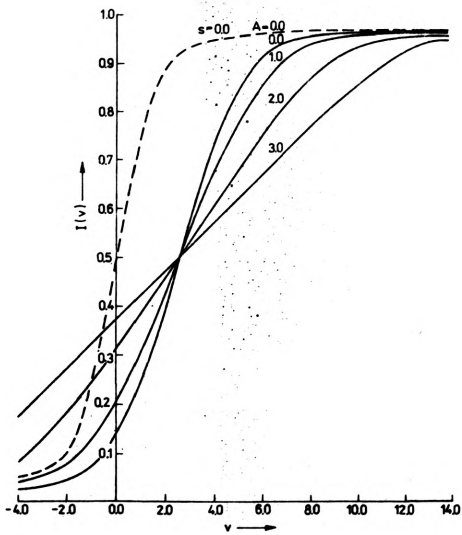


Fig. 6. The same as in Fig. 2, but for  $s = 5.0$

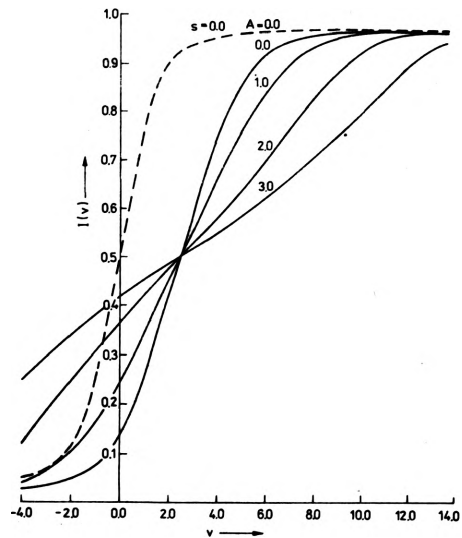


Fig. 7. The same as in Fig. 3, but for  $s = 5.0$

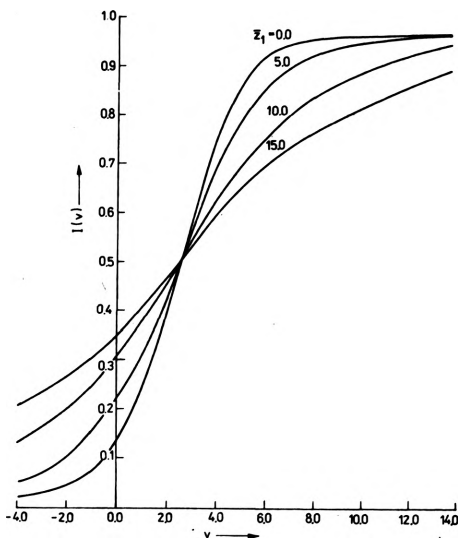


Fig. 8. The same as in Fig. 4, but for  $s = 5.0$

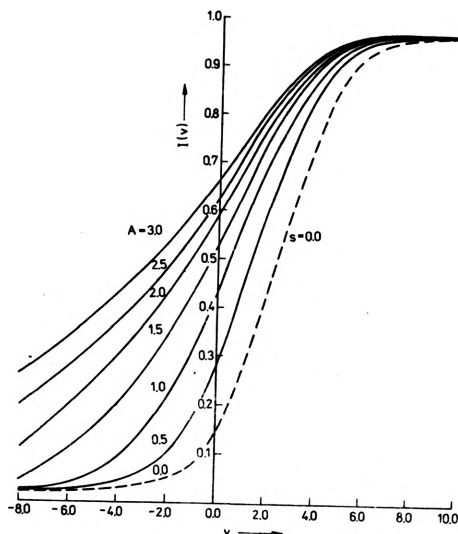


Fig. 9. The same as in Fig. 5, but for  $s = 5.0$

vibrations and parabolic image motion, respectively. Figures 6-9 show the same results for  $s = 5.0$ . Results for  $s = 10.0$  have also been calculated, but not presented here. In some cases results for an ideal edge have been marked by dotted curves for comparative reasons. Figure 10(a-c) shows the behaviour of the edge gradient for  $s = 5.0$ . Figure 11 shows typical isophotes or the lines of constant flux density for  $s = 5.0$ . Examples of the relief of flux density, i.e.,  $I(v)$ ,  $A$  and  $v$  relationship, in the degraded edge image for linear, transverse and parabolic motions have been shown in Fig. 12(a-c). The general trend of the results in the three cases of linear motion and

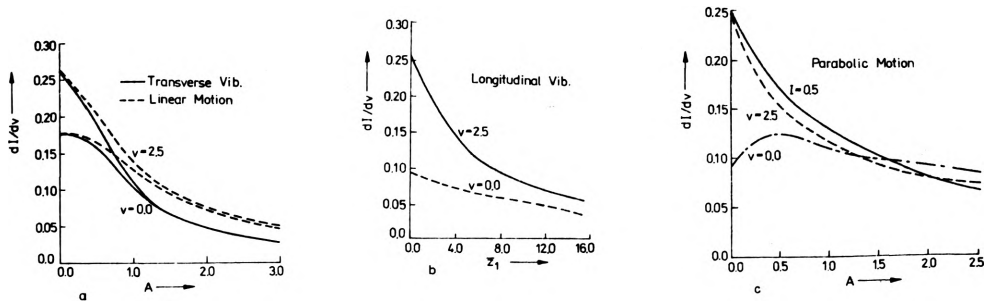


Fig. 10. Edge gradient for  $s = 5.0$  in presence of linear motion, transverse (a) and longitudinal (b) vibrations, and parabolic motion (c)



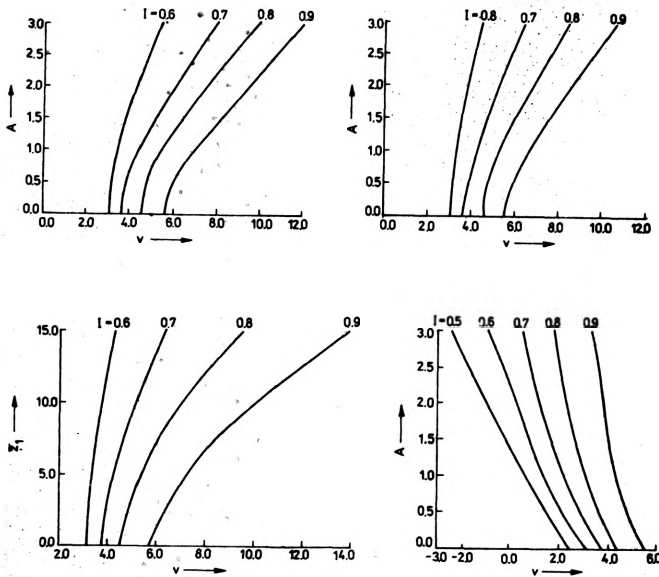


Fig. 11. Isophotes for  $s = 5.0$  in presence of linear motion, transverse and longitudinal vibrations, and parabolic motion

transverse longitudinal vibrations is the same. Therefore, in what follows the results of these three types of motion have been discussed collectively. Important conclusions from our investigations may be summarized as follows:

i) The slope of the intensity distribution curves at  $v = s/2$  has the highest value for the motion free case and is decreased as the amount of motion increases. It also decreases with the increasing amount of degradation. This can be easily inferred from Figs. 2-9.

ii) The edge spread function is always equal to 0.5 at  $v = s/2$  irrespective of the amount and type of image motion if the phase part in Eq. (10) is neglected. The position of half intensity level shifts towards the right with the increasing amount of degradation. The values of intensity for negative values of  $v$  cannot be calculated by the common relation  $I(-v) = 1.0 - I(v)$ . This relation, however, holds good, provided the origin is shifted to the position  $v = s/2$ . As the amount of motion increases, the intensity in the tail of the curve increases and the maximum intensity equal to unity is reached at higher values of  $v$ .

iii) The behaviour of edge gradient is somewhat similar to the variation observed while passing from coherent to the incoherent cases through different stages of partially coherent illumination; the dif-

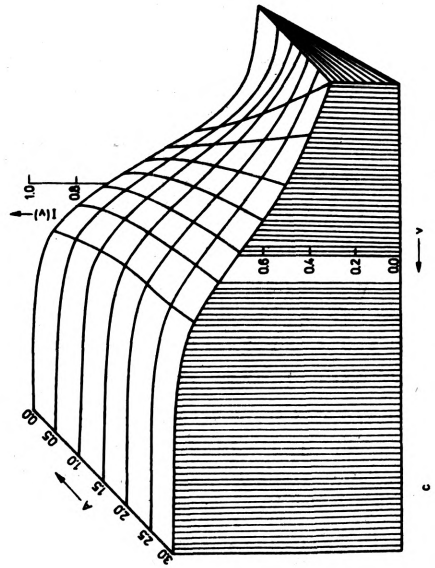
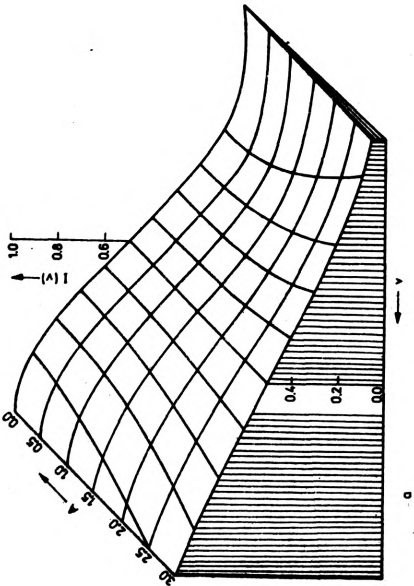
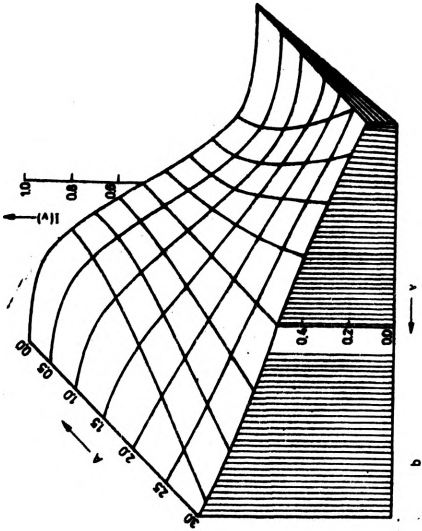


Fig. 12. Relief of flux density for  $s = 5.0$  in presence of linear motion (a), transverse vibrations (b), and parabolic motion (c)

ference is that the variation in the presence of image motion is larger than in the case of partial coherence for the same amount of degradation of the edge.

iv) It is also inferred from the figures for edge gradient that transverse vibrations are more deleterious than linear motion or longitudinal vibrations. For lower values of image motion parameter  $A$  or  $\bar{E}_1$ , combined with higher amount of degradation, the image may resemble that of a disk of larger diameter and may lead to misinterpretation of results.

v) It is inferred from Figs. 5 and 9 that in the presence of parabolic motion, the edge spread function is not equal to 5.0 and  $v = v/s$  as in other cases. This is so because the transfer function for parabolic image motion is complex valued having both a real and an imaginary part. It is this phase part which makes it difficult to locate the geometrical edge in the image. For example, for  $A = 2.0$ , the intensity in the image of an edge for  $s = 1.0$  at  $v = 0.5$  is 0.835 and in the image of an edge for  $s = 5.0$  its value at  $v = 2.5$  is 0.81; whereas if an intensity equal to 0.5 is looked for, the geometrical edge will be incoherently predicted because this value of intensity occurs at  $v = -2.8$  for  $s = 1.0$  and at  $v = -1.0$  for  $s = 5.0$ .

As can be inferred from Fig. 10c the edge gradient at  $v = s/2$  and at points where  $I(v) > 0.5$ , decreases with the increasing amount of motion. However, the edge gradient at  $v = 0.0$  shows a different behaviour. It increases initially and goes up to some maximum value for a small degradation of the edge. It appears to be maximum at  $A = 0.5$  and then decreases. This clearly indicates that the shape of the edge should be duly considered. If the edge is not ideal but suffers from degradation, then the edge gradient at geometrical edge (i.e., at  $v = 0.0$ ) will give misleading results as it does not decrease monotonically with the increasing amount of motion. Therefore, the knowledge of the amount of imperfection due to degradation seems to be of significant importance in the correct interpretation of the results of the edge trace analysis.

#### 4. Discussion of the accuracy in the numerical evaluation of the integrals

As already mentioned, the functions/integrands which have been evaluated are oscillatory in nature. The Gauss quadrature method is good for OTF calculations [32] and it gives good accuracy with 20 points. But, in the imaging calculations one must use more points say up to 50. BARAKAT [32] has discussed in detail the merits and demerits of various computational schemes and we need not go into this discussion here.

#### References

- [1] JENSEN N., Optical and Photographic Reconnaissance Systems, John Wiley and Sons, New York 1968.
- [2] FOUCHE C., [In] Space Optics, Eds. A. Maréchal and G. Coustes, Gordon and Breach, New York 1974.
- [3] WETHERELL W.B., Proc. SPIE 28 (1972), 45.
- [4] WETHERELL W.B., [In] Space Optics, Proc. of Ninth ICO Conference, Eds. B.J. Thompson, R.R. Shannon, Natl. Acad. Sci. Wash. D.C., 1974, p. 55.
- [5] ABOUTALIB A.O., MURPHY M.S., SILVERMAN L.K., IEEE Trans. Autom. Control. 22 (1977), 294.
- [6] PARIS D.P., Image Simulation Program (IMSIMI), Code V, Optical Research Associates, Pasadena, California, 1975.
- [7] WOLF P.R., Elements of Photogrammetry, McGraw-Hill Book Co., New York 1974.
- [8] MCFADDERN W.C., Proc. SPIE 19 (1976), 51.
- [9] KIDD R.H., WOLFE R.H., IBM J. Res. Dev. 20 (1976), 29.
- [10] WELCH R., Photogram. Eng. and Remote Sensing 43 (1977), 709.
- [11] SINGH K., JAIN N.K., Nouv. Rev. Opt. 3 (1972), 309.
- [12] SINGH R.N., SINGH K., CHANDRA A., Ind. J. Phys. 49 (1975), 28.
- [13] SINGH K., RATTAN R., MAGGO J.N., Appl. Opt. 44 (1975), 500.
- [14] LEVI L., Applied Optics, A Guide to Optical System Design, Vol. II, John Wiley and Sons, New York 1980.
- [15] PHAUJDAR S., JORDER M.K., SOM S.C., J. Opt. (India) 6 (1977), 68.
- [16] MAHAJAN V.N., Appl. Opt. 17 (1978), 3329.
- [17] SINGH K., DHILLON H.S., Atti. Fond. G. Ronchi 24 (1969), 462.

- [18] NAGEL M.R., Evaluation of Motion Degraded Images. Proc. of a Seminar Held in Cambridge, Mass. Dec. 3-5, 1968, NASA, Wash. D.C. 1969.
- [19] WELFORD W.T., [In] Advances in Optical and Electron Microscopy, Vol. II; Eds. R. Barer, V.E. Coslatt, Academic Press, London 1968.
- [20] BARAKAT R., J.Opt. Soc.Am. 55 (1965), 1217.
- [21] BARAKAT R., Opt. Acta 27 (1980), 847.
- [22] RATTAN R., SINGH K., J. Opt. (India) 3 (1974), 46.
- [23] SHEPPARD C.J.R., CHOUDHURY A., Opt. Acta 24 (1977), 1051.
- [24] GUPTA A.K., SINGH K., Microscop. Acta 80 (1978), 313.
- [25] WILSON T., Appl. Opt. 22 (1980), 119.
- [26] KINZLY R.E., J.Opt.Soc.Am. 55 (1965), 1002.
- [27] KINZLY R.E., J.Opt.Soc.Am. 56 (1966), 9, 526.
- [28] KINZLY R.E., J.Opt.Soc.Am. 62 (1972), 387, 1370A.
- [29] SCOTT R.M., Photo Sci. Eng. 3 (1969), 201.
- [30] LOHMAN A., PARIS D.P., Appl. Opt. 4 (1965), 393.
- [31] SOM S.C., J.Opt.Soc.Am. 61 (1971), 859.
- [32] BARAKAT R. [In] The Computer in Optical Research, Eds. B.R. Frieden, Springer-Verlag, Berlin, New York. Heidelberg 1980.

Received June 20, 1981  
in revised form January 18, 1982

#### ДИФРАКЦИОННОЕ ОТОБРАЖЕНИЕ ДЕГРАДИРОВАННОГО КРАЯ ВСЛЕДСТВИЕ ДВИЖЕНИЯ ИЗОБРАЖЕНИЯ

Теоретически исследованы дифракционные изображения некогерентно освещенного края в условиях движения изображения. Отдельно исследованы деградационные эффекты при продольных и поперечных синусоидальных колебаниях, а также при линейных и параболических движениях изображения. Рассчитано распределение освещенности в дифракционных изображениях при использовании функции переноса. Результаты представлены графически. Отмечено, что эффект деградации края является важным при оценке влияния эффектов различного типа движений изображения на качество работы оптических систем.